Available online at www.sciencedirect.com

SciVerse ScienceDirect

www.elsevier.com/locate/matchar

Novel EBSD preparation method for Cu/Sn microbumps using a focused ion beam

Tao-Chi Liu[a], Chih Chen[a], Kuo-Jung Chiu[b], Han-Wen Lin[a], Jui-Chao Kuo[c,*]

[a]National Chiao Tung University, Department of Materials Science and Engineering, Hsinchu 30010, Taiwan, ROC
[b]Integrated Service Technology Inc., No. 19, Pu-ding Rd., Hsinchu 30072, Taiwan, ROC
[c]National Cheng Kung University, Department of Materials Science and Engineering, Tainan, Taiwan, ROC

ARTICLE DATA

Article history:
Received 2 June 2012
Received in revised form
23 August 2012
Accepted 1 September 2012

Keywords:
Focused ion beam (FIB)
Intermetallic compound
Sample preparation
Image quality
Electron backscatter diffraction (EBSD)

ABSTRACT

We proposed a novel technique developed from focused ion beam (FIB) polishing for sample preparation of electron backscatter diffraction (EBSD) measurement. A low-angle incident gallium ion beam with a high acceleration voltage of 30 kV was used to eliminate the surface roughness of cross-sectioned microbumps resulting from mechanical polishing. This work demonstrates the application of the FIB polishing technique to solders for a high-quality sample preparation for EBSD measurement after mechanical polishing.
© 2012 Elsevier Inc. All rights reserved.

1. Introduction

Solders, a kind of very soft material, are widely used as joints to fuse the metal pads together for electrical connection in electronic devices. The conventional metallographic sample preparation of solder joints is the mechanical polishing, which usually results in critical preparation damages to the soft surfaces. The solid surface can be modified by an ion beam for the surface topographies [1]. Currently, damage-free ion beam techniques of the cross-sectional polisher (CP) are developed to improve the quality of sample preparation since the techniques are able to section large materials into 1 mm-wide pieces [2,3]. The damages induced by the ions can be optimized for ion etching is parallel to the cross-sectioned surface. Nevertheless, the acceleration voltage of the CP beam source, which is in the range of 2–6 kV, results in a relatively slow milling rate that makes CP sample preparation time-consuming.

Most failures of solder joints occur at the interfaces of tiny structures, and these failures reduce the product reliability [4–8]. The interfacial properties of solder joints are determined by the formation of intermetallic compounds (IMCs) consisting of more than two metallic elements, whose reactions involve a liquid or solid phase. Thus, the reaction mechanism is extremely complex. Recently, in addition to TEM, the electron backscatter diffraction (EBSD) technique has been widely applied to the investigation of microstructures in solder joints to analyze the complex interfacial reactions [9–11]. EBSD, combined with scanning electron microscopy, has been used to analyze grain microstructures and their crystallographic orientations [12–14]. Here, the backscattered electrons are diffracted and collected to produce Kikuchi patterns. The quality of EBSD patterns (EBSPs) is extremely sensitive to the surface quality of specimens, such as flatness and completeness. Therefore, a flat surface, free of critical residual preparation damage, is required for EBSPs with high-quality pattern indexes. The CP technique can provide sample preparations with better qualities to satisfy the requirement of EBSD. When the dimensions of solder joints continuously shrink down to

* Corresponding author.
E-mail address: jckuo@mail.ncku.edu.tw (J.-C. Kuo).

1044-5803/$ – see front matter © 2012 Elsevier Inc. All rights reserved.
http://dx.doi.org/10.1016/j.matchar.2012.09.002

tens of micrometers, i.e. micro-bumps, CP is insufficient to access a specific region or individual bump structure.

In the last few years, the focused ion beam (FIB) technique has been used for EBSD sample preparation, especially for 3D EBSD measurement, where the ion beam size is in nanometers. Matteson et al. [15] prepared Si and Cu samples by tilting the samples' surfaces toward the FIB direction and reached a highly improved EBSP quality. West and Thomson [16] used combined EBSD/EDS tomography in a dual-beam FIB to study the interdiffusion in a nickel-based superalloy. Xu et al. [17] combined the use of FIB with EBSD on sequentially milled slices of iron threads and Ni–Si alloys to obtain crystallographic information of microstructures. Konrad et al. [18] used 3D EBSD–FIB to investigate the orientation gradients around a hard Laves phase in an Fe_3Al alloy. However, the FIB technique applied to solder bumps was absent.

CP, FIB and mechanical polishing methods are widely applied to the sample preparations on solders; moreover, simply using CP or FB polishing can spend a lot of time and cost. In this study, we propose an EBSD sample preparation using FIB polishing directly after the cross-section of the microbumps is mechanically polished. This combination method can reduce the cost and time. In addition, this combination method is able to polish a specific area while mechanical polishing cannot. At the beginning of this study, FIB and CP techniques were employed to polish the cross-section of Cu/Ni/solder microbumps directly after mechanical polishing. After comparing the efficiency and ability of FIB and CP polishing, the combination of FIB and mechanical polishing was finally performed on Cu UBM for EBSD analysis. Lastly, this methodology was applied to the microstructural modification of multiphase IMCs in thermally aged Cu/Sn microbumps.

2. Experimental

Three types of samples were employed in this study: Cu/Ni/solder microbumps, Cu underbump metallization (UBM), and thermally aged microbumps consisting of five metal/IMC layers. After all the samples had been firstly fixed with molding compounds, the cross sections of the samples were grinded with SiC 1000 and 4000 grit and polished with 0.05 mm alumina suspensions. We used an optical microscope after every step of mechanical polishing in order to observe the whole microbump structure. After the above processes, the remaining molding on the chip was thinned to avoid obstruction of the incident ion beam. FIB and CP were then used to polish the sample surface further. In the FIB polishing case, a Helios NanoLab™ 600 was used for low-angle polishing, which requires 30 kV gallium ions combined with beam currents of 21 nA and 100 pA. In addition, a high-performance Sidewinder ion column that combines high resolution with low voltage provides fast and precise ion milling which prevents damages to the cross-sections during operations and provides high-resolution imaging quality.

The geometrical positions of the sample and the incident ion beam during polishing are shown in Fig. 1. The polished surfaces of the sample and the incident ion beam were tilted 47° and 52° from the horizontal position respectively. That is, the angle between the ion beam and the sample surface is 5°. This condition allows the ion beam to remove a very thin surface layer from the sample and to eliminate scratches and roughness caused by mechanical polishing. The polishing procedure is shown in Fig. 2. First, a high beam current of 21 nA was used for fast removal of the scratches on the surfaces; however, many slight scratches were induced by ion etching. The scratches were soon formed after FIB polishing using high beam current initially, and this phenomenon was so called the curtaining effect. The surface damage can refer to the work in [19]. Therefore, the ion-induced scratches were further polished with a low beam current of 100 pA. After polishing, to obtain a high contrast image of the grain microstructure, an ultra-low beam current of 9.7 pA was employed for the FIB imaging. Moreover, the surface damage was minimized during the microstructure observation.

In addition to the FIB polishing, conventional cross-sectional polishing performed by JEOL SM09010 using an argon ion source was also applied to a cross-sectional sample preparation of the microbumps at 6 kV. A 500 μm diameter beam was chosen with the aid of a metal shield plate to provide a straight cross section perpendicular to the surface of the specimen.

EBSD analysis was performed on the FIB-polished samples using a JEOL 7001F field emission electron microscope with an EDAX/TSL EBSD system at 20 kV. The analyzed area was 90×30 μm^2 with a step size of 50 nm.

3. Results and Discussion

3.1. Comparison of the FIB and CP Polishing Processes

Fig. 3(a) shows the structure of the FIB polished Cu/Ni/solder microbumps where the marked circle area with a width of 25 μm is chosen for fine FIB polishing, as shown in Fig. 3(b). No surface damage is observed on the surfaces at both sides of the

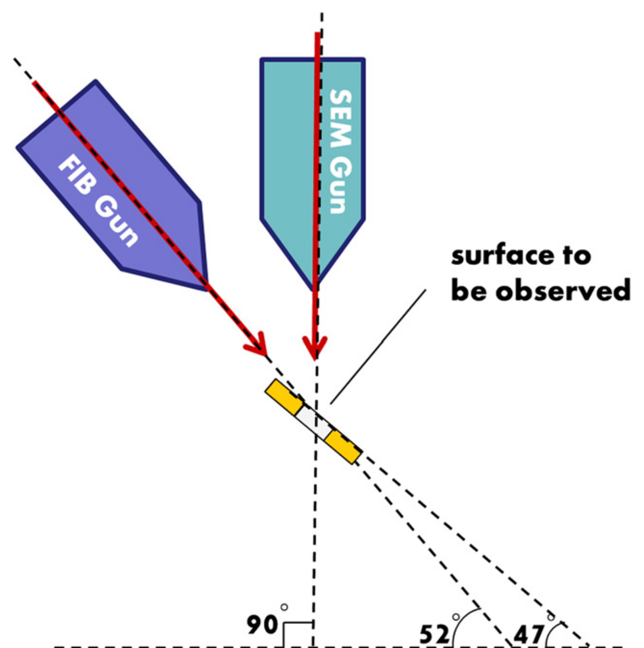

Fig. 1 – Schematic illustration of the low-angle FIB polishing method.

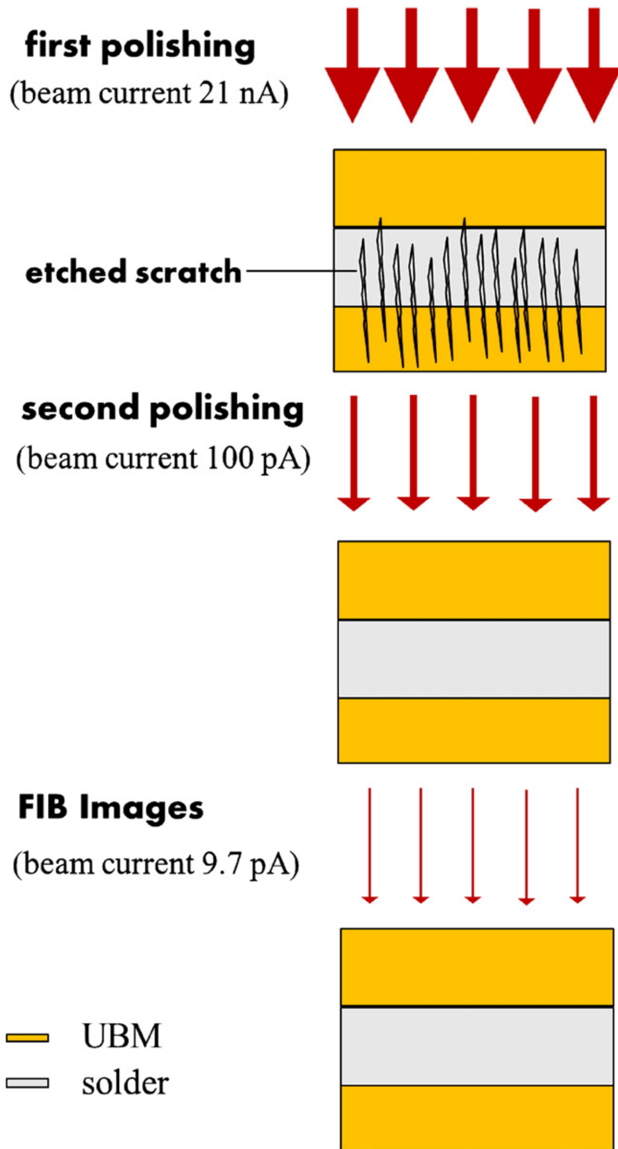

Fig. 2 – Schematic illustration of the FIB polishing procedure.

organic compound, and the solder has a low melting point, as shown in Fig. 3(a). Fig. 3(b) shows the clear microstructure of Cu, Ni, IMC, and the solder layers. The degrees of contrasts reveal the crystallographic orientation. Thus, the contrast differences make the IMC layers obvious, which can be used to estimate the growth rate of the IMCs for the reaction kinetics. Furthermore, the thermolabile organic compound layer remains undamaged after being ion polished. Conventionally, preparing the cross section of the multiple phases is extremely difficult due to the different mechanical properties of the multiple phases, such as those consisting of soft or hard materials. Therefore, this polishing method provides an alternative for the preparation of high-quality and almost distortion-free sample surfaces.

Fig. 4(a) shows the FIB images of the CP polished cross sections of the Cu/Ni/solder microbumps. Four microbumps marked in the left area of the figure are not very well polished because of the incident aberration of the ion beams. Moreover, Fig. 4(a) shows that the cross section is not perpendicular to the sample surface. Fig. 4(b) shows the FIB image of one microbump in a well-polished region where the grain microstructure of Cu is not clear while the clear step height occurs in the interfaces between the IMCs and the solder. In addition, polishing damages are also found in the interface of the solder and the organic compound. To compare with CP polishing, Fig. 4(c) shows the SEM image of a mechanically polished microbump and a clear difference in height between the two phases is observed in the microbump. The surface damage induced by FIB can refer to the work by Kowalski et al. [19].

Conventionally, ion-beam cross sectioning is quite a time-consuming process. The low milling rate makes the application to large-area samples ineffective and expensive. On the other hand, the low-angle FIB polishing technique allows precisely controlled removal of ultra-thin slices of the substrate; thus, the total process time is only 15 min for a $90\times30\ \mu m^2$ cross-sectional area. Further, its cross-sectioning quality is much better than that of other conventional sample preparation techniques.

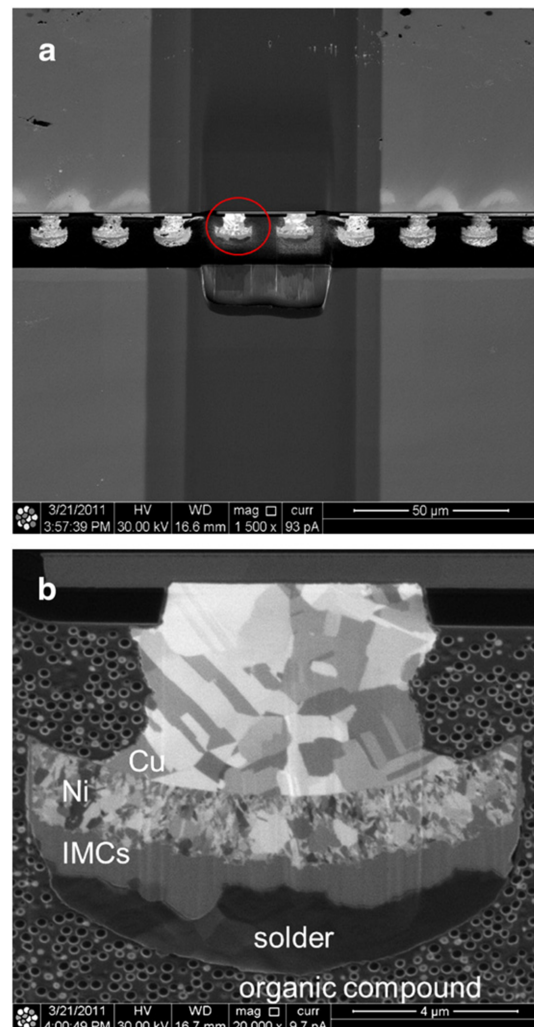

Fig. 3 – (a) FIB image of Cu/Ni/solder microbumps after ion-beam polishing, and (b) magnified FIB image of (a).

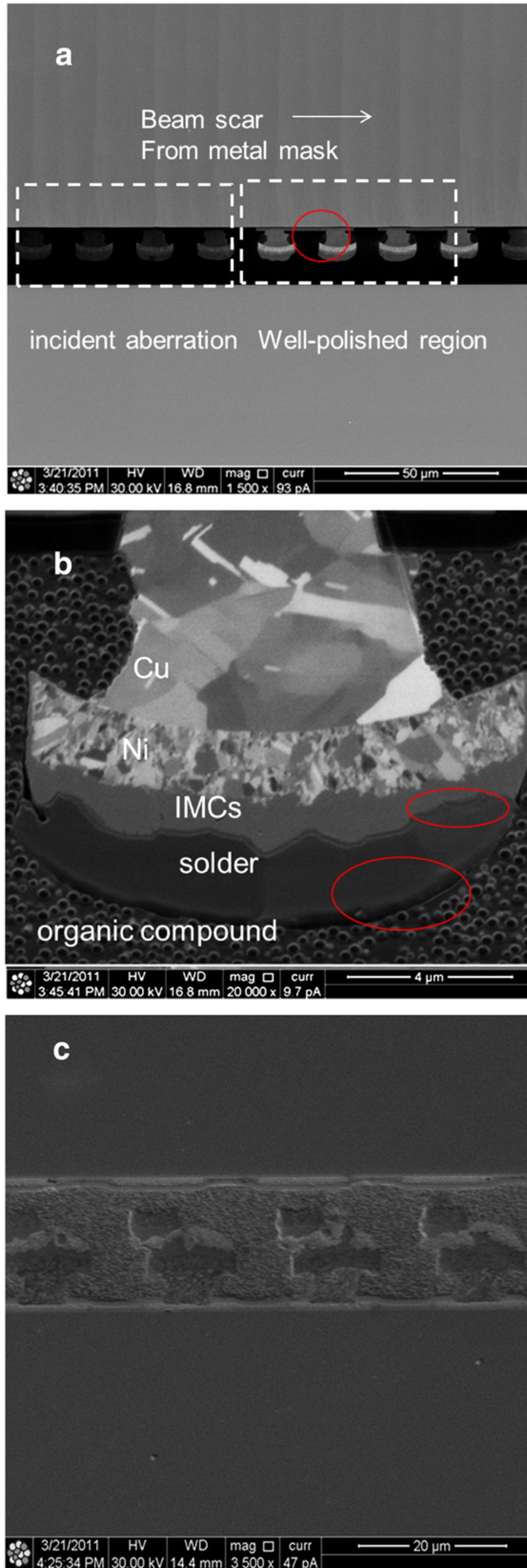

Fig. 4 – (a) FIB image of Cu/Ni/solder microbumps after CP polishing, and (b) magnified FIB image of (a), where an obvious step height is formed on the interface of the IMCs/solder and solder/organic compounds.

3.2. *Polishing Ability of FIB*

If the incident angle between the incident beam and the surface is more than 5°, the surface milling will certainly occur during the FIB polishing process. In contrast, if the incident angle is less than 5°, the ion beam may almost parallel the sample surface and the polishing process will not occur. Therefore, during the FIB polishing process, the incident angle must be at 5°, and that is so called the low-angle polishing technique.

After fixing the incident angle, the next step is to make sure of the size of the effective polish area. Fig. 5(a) shows the FIB image of the Cu UBM surface after being low-angle polished. It is observed that the difference in the surface roughness is obvious as a function of distance. In the distance of 40 μm measured from the top the polished area is a clear microstructure with some scratches which are formed after being FIB polished with high beam current initially. This region is called an ideal polish area. When the distance is

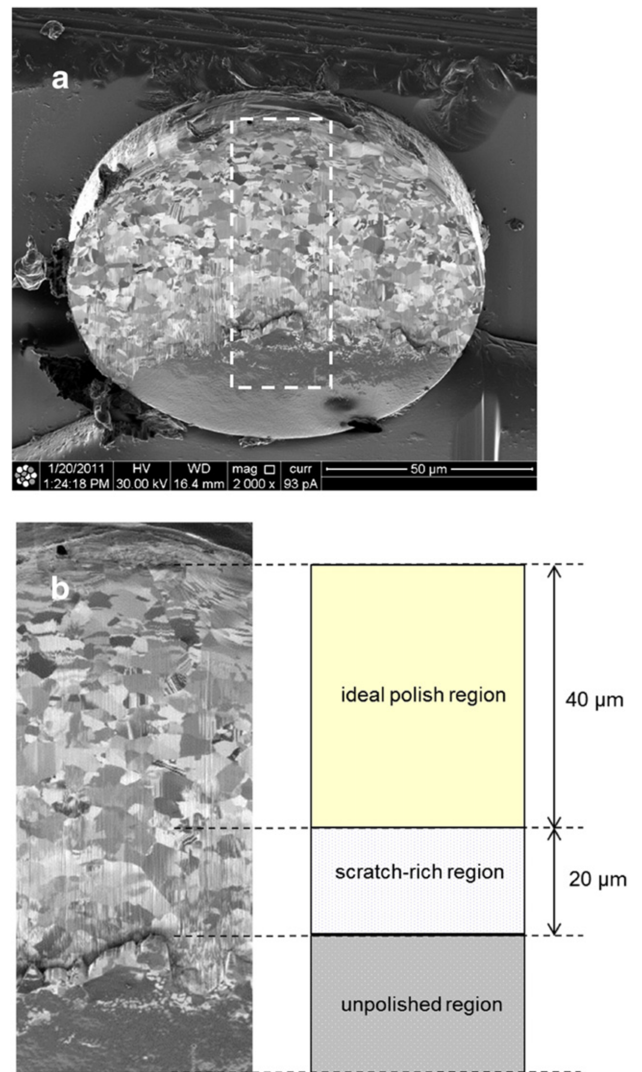

Fig. 5 – (a) FIB image of Cu UBM after FIB polishing, and (b) schematic illustration of a polished surface containing three regions, namely an ideal polished region, a scratch-rich region, and an ion-induced damage region.

between 40 and 60 μm, a lot of serious scratches are found in the region which is indicated as scratch-rich. In the case of the distance longer than 60 μm, the ion beam directly digs the substrate and the surface polishing cannot continue. Thus, the effective polish region in this case is within 40 μm measured from the top of the polished area. The size of the effective polish area depends on the material and the operation parameters. The height of this area is determined by the curtaining effect which depends on the material, its microstructure and its crystal orientation. The longest curtain-free distance achieved is longer than 40 μm on an FeNi sample [13].

3.3. Application of FIB Polishing to Multiple Phases of Microbumps

Application of a conventional mechanical polishing process to the preparation of a multiphase component sample has been a great challenge. For instance, Cu is softer than IMCs, and mechanical polishing results in step height on the interface and scratches on the soft base. The quality of the Kikuchi patterns of the EBSD measurements strongly depends on the quality of the sample surface, such as the roughness and residual stress. Therefore, EBSD analysis is used to investigate the surface quality after the FIB polishing.

The Cu/SnAg solder bonded to a Cu microbump is aged at 150 °C for 500 h to form multiple phases consisting of Cu, Cu_3Sn, Cu_6Sn_5, and Ag_3Sn. Fig. 6 presents the marked Kikuchi patterns of Cu, Cu_3Sn, Cu_6Sn_5 and Sn, respectively. The raw Kikuchi patterns of Cu, Cu_3Sn, Cu_6Sn_5 and Sn obtained from EBSD measurement are indexed as cubic, orthorhombic, hexagonally close-packed and monoclinic, respectively. At the same time, the chemical composition of Cu, Cu_3Sn, Cu_6Sn_5 and Sn is identified by an energy-dispersive detector (EDS). Fig. 7(a) shows the FIB image of the FIB-polished microbump consisting of a typical multiphase microstructure. The magnified FIB image of the multiphase microstructure in Fig. 7(a) is shown in Fig. 7(b), which clearly shows four

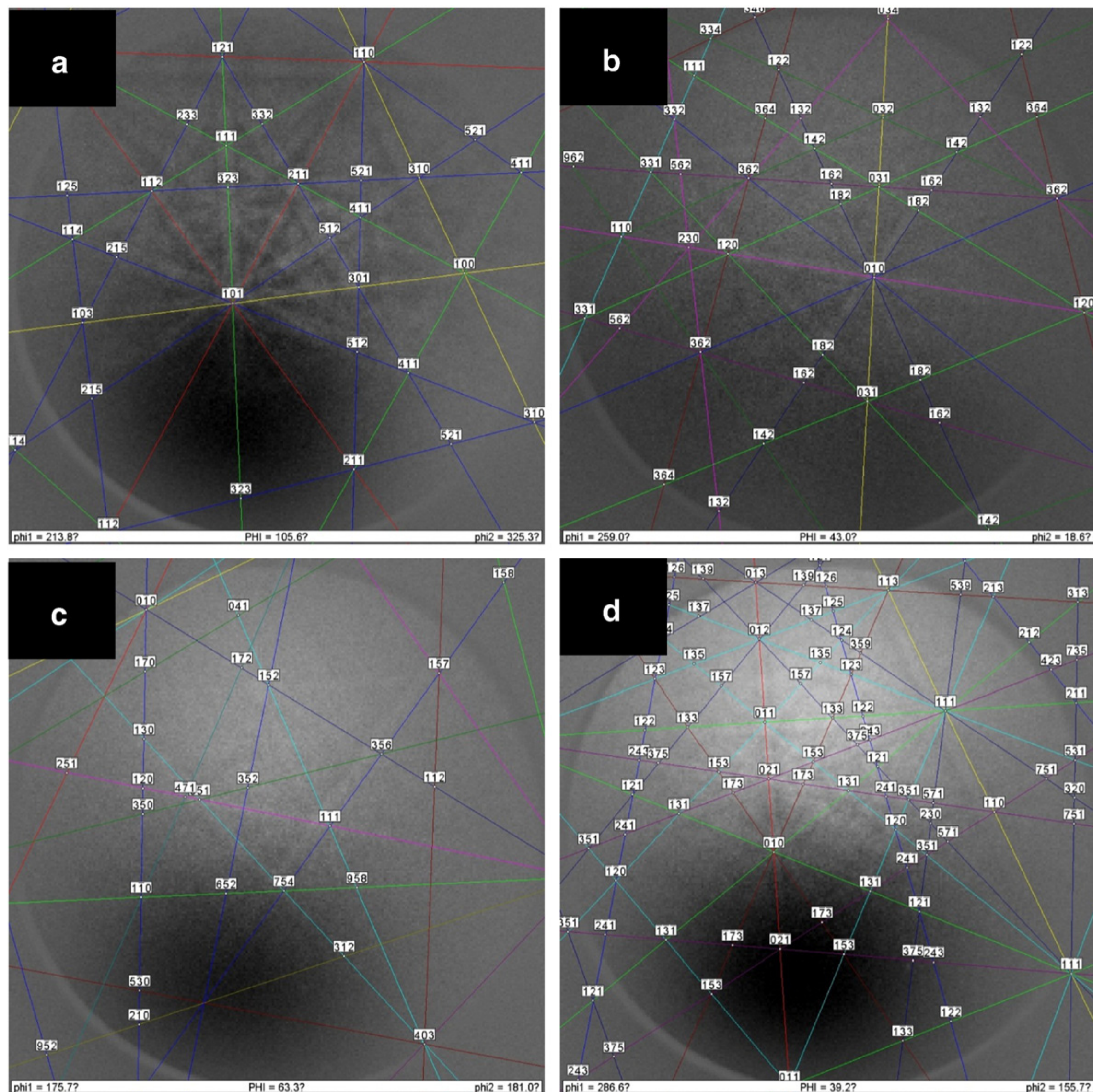

Fig. 6 – EBSD pattern with bands and result of indexing for (a) Cu, (b) Cu_3Sn, (c) Cu_6Sn_5 and (d) Sn.

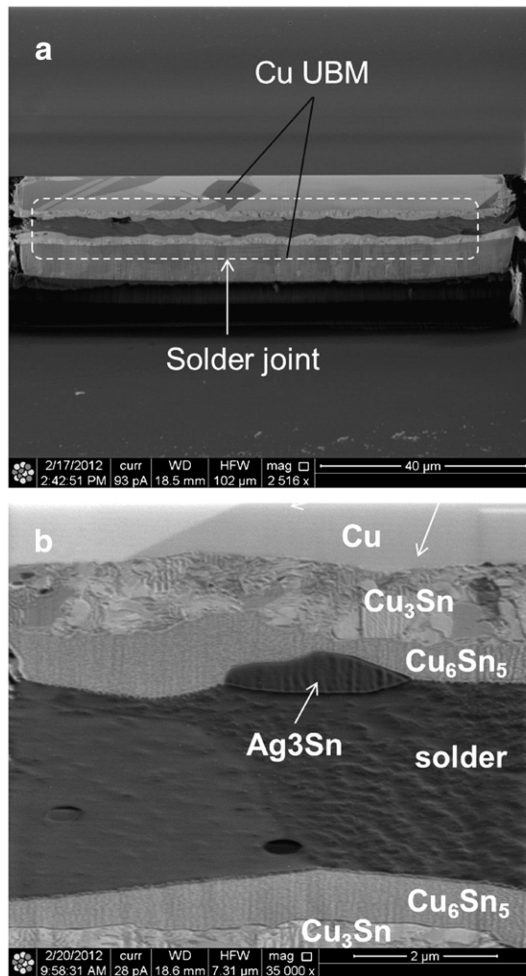

Fig. 7 – (a) FIB image of a thermally aged Cu/Sn microbump after FIB polishing and (b) magnified FIB image of (a).

layers of Cu, Cu_3Sn, Cu_6Sn_5, and solder according to the contrasting differences whose phases are analyzed by EBSD.

In addition to the FIB image, Fig. 8 shows the IPF map of the FIB cross-sectioned sample obtained from EBSD, which consists of four phases, namely, Sn, Cu_3Sn, Cu_6Sn_5, and Ag_3Sn. After a 500 h solid-state reaction, the Cu_6Sn_5 layer is formed and the Cu_6Sn_5 phase is decomposed into Cu_3Sn. Fine grains of Cu_3Sn are located between the Cu and Cu_6Sn_5 layers. Tu [1] proposes that the grain boundaries act as either a vacancy source or a vacancy sink. The vacancy expansion resulting in Kirkendall voids on the interface of Cu and the solder has been the most serious constructional problem at the solder joint.

4. Conclusion

The proposed FIB polishing technique has been successfully developed to prepare samples for EBSD measurement of bonded microbumps. A low-angle incident ion beam is employed to produce a flat cross-sectional surface free of damages resulting from mechanical polishing. It is a fast and low-cost process that enables polishing of a large surface of multiple phases to use a high beam voltage.

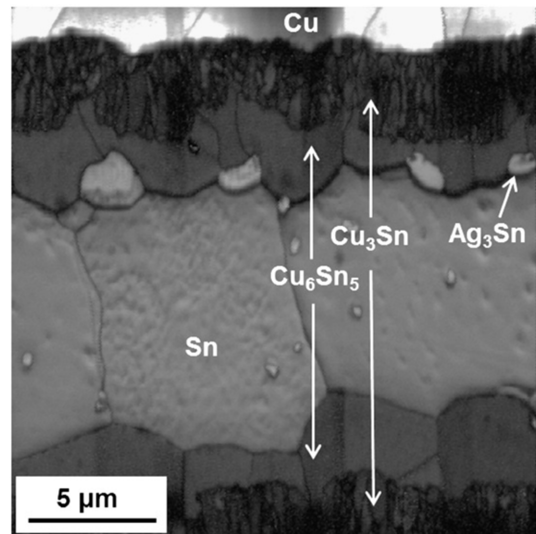

Fig. 8 – IPF map of a thermally aged Cu/Sn microbump overlapped with grain boundaries obtained from EBSD measurement after FIB polishing.

Acknowledgments

The authors would like to thank the National Science Council (ROC) through grant no. NSC 100-2628-E-006-024-MY3, and the Center for Micro/Nano Science and Technology for providing the facilities.

REFERENCES

[1] Kowalski ZW, Wilk J, Martan J. Electron backscatter diffraction of grain and subgrain structures — resolution considerations. Vacuum 2009:S208-13.
[2] Erdman N, Campbell R, Precise Asahina S. SEM cross-section polishing via argon beam milling. Microsc today 2006:22-5.
[3] Wang Y, Ohnuki S, Hayashi S, Narita T. Submicron structure of rhenium-base diffusion barrier coating layer on a nickel-base superalloy. Mater Trans 2007;48-3:526-30.
[4] Tu KN. Solder joint technology materials, properties, and reliability. New York: Springer Science; 2007.
[5] Chen HY, Chen C, Tu KN. Failure induced by thermomigration of interstitial Cu in Pb-free flip chip solder joints. Appl Phys Lett 2008;93:122103.
[6] Huang YS, Hsiao HY, Chen C, Tu KN. The effect of a concentration gradient on interfacial reactions in microbumps of Ni/SnAg/Cu during liquid-state soldering. Scr Mater 2011;66:741-4.
[7] Yu CY, Duh JG. Stabilization of hexagonal Cu6(Sn, Zn)5 by minor Zn doping of Sn-based solder joints. Scr Mater 2011;65: 783-6.
[8] Ventura T, Terzi S, Rappaz M, Dahle AK. Effects of Ni additions, trace elements and solidification kinetics on microstructure formation in Sn–0.7Cu solder. Acta Mater 2011;59:4197-206.
[9] Gong JC, Liu CQ, Conway PP, Silberschmidt VV. Evolution of CuSn intermetallics between molten SnAgCu solder and Cu substrate. Acta Mater 2008;56:4291-7.
[10] Chen D, Ho CE, Kuo JC. Current stressing-induced growth of Cu_3Sn in Cu/Sn/Cu solder joints. Mater Lett 2011;65:1276-9.

[11] Chen WM, Yang TL, Chung CK, Kao CR. The orientation relationship between Ni and Cu6Sn5 formed during the soldering reaction. Scr Mater 2011;65:331-4.
[12] Randle V. Microtexture determination and its applications. 2nd ed.Maney; 2008.
[13] Schwartz AJ, Kumar M, Field DP. Electron backscatter diffraction in materials science. 2nd ed.Springer; 2000.
[14] Abou-Ras D, Koch CT, Küstner V, van Aken VA, Jahn U, Contreras MA, et al. Grain-boundary types in chalcopyrite-type thin films and their correlations with film texture and electrical properties. Thin Solid Films 2009;517: 2545-9.
[15] Matteson TL, Schwarz SW, Houge EC, Kempshall BW, Giannuzzi LA. Electron backscattering diffraction investigation of focused ion beam surfaces. J Electron Mater 2002;30-1:33-9.
[16] West GD, Thomson RC. Combined EBSD/EDS tomography in a dual-beam FIB/FEG–SEM. J Microsc 2009;233-3:442-50.
[17] Xu W, Ferry M, Mateescu N, Cairney JM, Humphreys FJ. Techniques for generating 3-D EBSD microstructures by FIB tomography. Mater Charact 2007;58:961-7.
[18] Konrad J, Zaefferer S, Raabe D. Investigation of orientation gradients around a hard Laves particle in a warm-rolled Fe_3Al-based alloy using a 3D EBSD–FIB technique. Acta Mater 2006;54:1369-80.
[19] Kowalski ZW, Wilk J, Martan J. Surface morphology of steel and titanium induced by ion beam bombardment — comprehensive analysis. Vacuum 2009;83:S208-13.